

Temperature dependent responsivity of quantum dot infrared photodetectors

S.Y. Wang ^{a,*}, M.C. Lo ^b, H.Y. Hsiao ^c, H.S. Ling ^b, C.P. Lee ^b

^a *Institute of Astronomy and Astrophysics, Academia Sinica, P.O. Box 23-141, Taipei 106, Taiwan*

^b *Department of Electronic Engineering, National Chiao Tung University, Hsin Chu 300, Taiwan*

^c *Institute of Opto-electronics Engineering, Chang Gung University, Tao Yuan 333, Taiwan*

Available online 20 November 2006

Abstract

Temperature dependent behavior of the responsivity of InAs/GaAs quantum dot infrared photodetectors was investigated with detailed measurement of the current gain. The current gain varied about two orders of magnitude with 100 K temperature change. Meanwhile, the change in quantum efficiency is within a factor of 10. The dramatic change of the current gain is explained by the repulsive coulomb potential of the extra carriers in the QDs. With the measured current gain, the extra carrier number in QDs was calculated. More than one electron per QD could be captured as the dark current increases at 150 K. The extra electrons in the QDs elevated the Fermi level and changed the quantum efficiency of the QDIPs. The temperature dependence of the responsivity was qualitatively explained with the extra electrons.

© 2006 Elsevier B.V. All rights reserved.

PACS: 85.60.Gz; 73.50.Pz

Keywords: Quantum dot; Intersubband; Infrared detector

1. Introduction

In the past decade, quantum dot infrared photodetectors (QDIPs) have been widely investigated with different structures and materials [1–3]. The three-dimensional confinement of the quantum dot structure provides the possibility to suppress the electron phonon interaction and relax the selection rule of intersubband transition in quantum well structures. Thus, QDIPs are of great potential to overcome the drawbacks of the commercialized QWIPs and become low cost, high temperature operation infrared detectors [4]. With the insertion of AlGaAs blocking layer, high performance QDIPs were successfully demonstrated in our previous work [5] and also by other groups [6,7].

Moreover, QDIPs with operation temperature higher than 200 K and even room temperature has been demonstrated with different device structures [8,9]. The encouraging results demonstrated the advantages of QDIPs at high operation temperature.

It has been noticed that the responsivity of QDIPs shows a very different behavior compared to that of QWIPs [10]. In QWIPs, the responsivity keeps almost constant at different device temperatures and changes linearly with the bias voltage for B–C type device. On the contrary, in QDIPs, the responsivity increases dramatically with both voltage and temperature. The stability of the responsivity with either temperature or voltage is crucial to provide a wide operation range in practical applications. However, only limited research has been done on this issue. Detailed analysis on the quantum efficiency considering the temperature dependent of the escape rate, the ground state population and excited carrier life time has been published [3]. The calculated quantum efficiency showed a small change

* Corresponding author. Tel.: +886 2 33652200x823; fax: +886 2 23677849.

E-mail address: sywang@asiaa.sinica.edu.tw (S.Y. Wang).

within a factor of 2 from 0 K to 150 K under a fixed voltage. It is much smaller than the measured responsivity change which varies by a factor of 10 within 100 K. Thus, other factors must be considered to explain the temperature dependence of the responsivity of QDIPs. Although it is observed that the current gain varies with the temperature, no detailed study was executed with the experimental data [10]. In this study, a detailed analysis of the responsivity was done based on the current gain measurement to explain the temperature dependence of the responsivity in QDIPs.

2. Basic characteristics of the sample

The sample was grown by Varian Gen II MBE machine on (100) GaAs semi-insulating substrate. Ten periods of InAs/GaAs QDs with 500 Å barriers were used in the active region. Each barrier consisted of 470 Å GaAs layer and 30 Å $\text{Al}_{0.2}\text{Ga}_{0.8}\text{As}$ current blocking layer that was supposed to partially cover the quantum dots. Fig. 1 shows the device structure and the band diagram of the active region. The detail function of the current blocking layer was explained in Ref. [5]. The active region was sandwiched by 5000 Å n-type contact layers. δ -Doped Si layer with concentration of $2 \times 10^{10} \text{ cm}^{-2}$ was inserted 20 Å before each QD layer to provide electrons in each QD. The size of the quantum dot is about 60 Å in height and 220 Å in radius by the examination of AFM. The QD density is about $1.7 \times 10^{10} \text{ cm}^{-2}$ which means the carrier density is about 1.2 electrons in each dot. Standard processing techniques were used to define the mesas and make ohmic contacts. AuGe contact ring is fabricated on the mesa top to allow the normal incident measurement.

The PL and inter-band photocurrent spectrum of the sample showed transition peaks at 1.13, 1.19, 1.42 eV with a FWHM around 50 meV. Comparing the infrared respon-

sivity peak ($6 \mu\text{m} \sim 205 \text{ meV}$) with the transition peaks, the transition could be deduced to be from the ground state to the bound excited state associated with the 1.42 eV transition peak. The photon excited carriers is about 70 meV lower than the GaAs band edge assuming a 70% energy discontinuity in the conduction band. The device characteristics at different temperatures were measured using a close cycled helium cryostat. In all measurements, the bottom contact is referred as ground. The dark current density is less than $1 \times 10^{-5} \text{ A/cm}^2$ at 77 K and 0.3 V. Fig. 2 shows the dark current activation energy at different voltages. The activation energy of the dark current is about 140 meV at low bias and decreases linearly with the increase of voltage. The decrease of the activation energy has been investigated to be from the tunneling process between the QD layers [11]. The low activation energy implies the impact ionization could happen at the high voltage region. Assuming a uniform electric field distribution across the device, the kinetic energy of the emitted carriers is higher than the activation energy when bias is larger than 0.9 V or -0.75 V . The multiplication process generates extra noise to the usual G–R noise and deteriorates the performance. In order to get the reasonable gain value, we limited the bias range between 0.9 V and -0.75 V in the following discussions. The photo-response of the devices were measured at different temperatures by a FTIR spectrometer, and calibrated by a 1000 K blackbody source under normal incident illumination. The device performance is very close to our previous result with a detectivity of $1 \times 10^{10} \text{ cm Hz}^{1/2}/\text{W}$ and responsivity of 0.2 A/W at 0.5 V and 77 K. Fig. 3 shows the responsivity of the sample at different temperatures and biases. As mentioned, the responsivity increases exponentially with voltage. As the temperature rose, the responsivity also increased dramatically from 40 K to 100 K and saturated after 100 K. Such dependence is quite different from what has been observed in QWIPs.

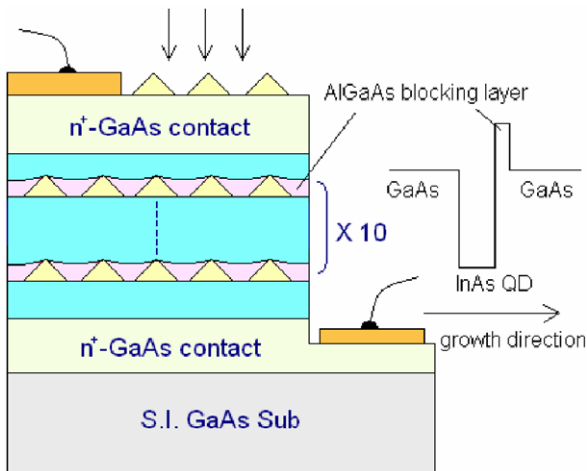


Fig. 1. The schematics of the device structure used in this study. Inset shows the band diagram of the QDs in the active region.

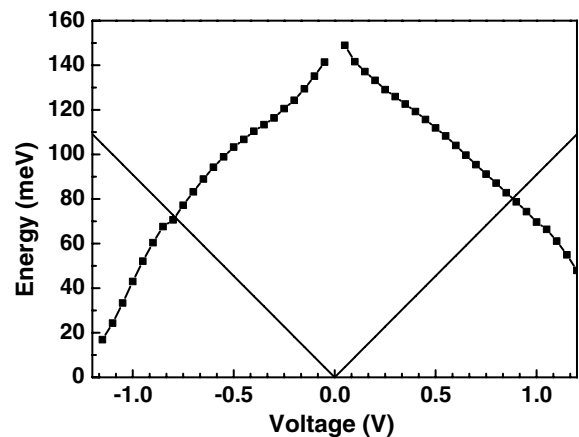


Fig. 2. The dark current activation energy at different voltages. The straight line shows the kinetic energy of electrons across one barrier under uniform electric field.

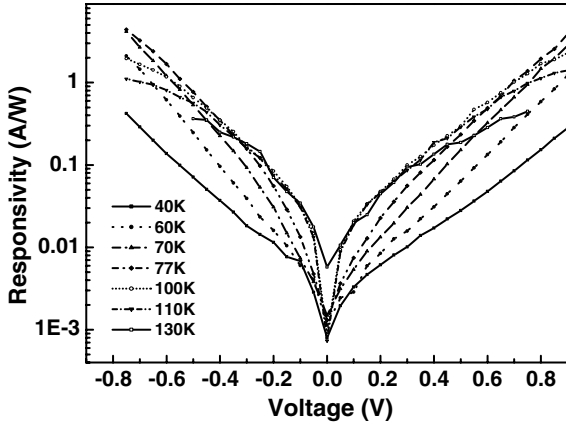


Fig. 3. The responsivity versus voltage at different temperatures.

3. Results and discussion

In order to investigate the temperature dependent of the responsivity, we measured the current gain and separated the quantum efficiency from the responsivity. The noise current of the device was measured at different temperatures and biases. The noise spectrum at 130 K is shown in Fig. 4. Similar to QWIPs, the noise spectrum showed a white noise feature and is dominated by the carrier generation and recombination process, i.e., G–R noise in QDIPs [10]. The relation between the G–R noise current and the current gain g is:

$$g = \frac{I_n^2}{4qI_d} \quad (1)$$

where I_d is the dark current, and I_n is the noise current. The current gain was calculated and plotted in Fig. 5. Due to the limit of the measurement system, noise current smaller than 1×10^{-13} A/Hz^{1/2} cannot be correctly measured. Thus, the current gain at lower biases with lower temperatures is not available. Obviously, the current gain has a similar trend as the responsivity does. The current gain increases more than 50 times from 70 K to 140 K. The carrier capture probability through the QD layer changed dramati-

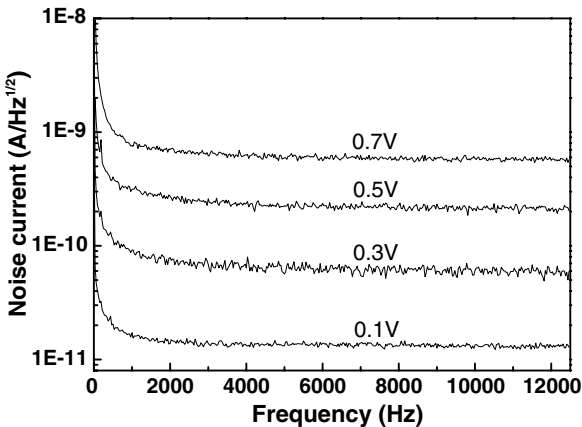


Fig. 4. The noise spectrum at 130 K and different bias voltages.

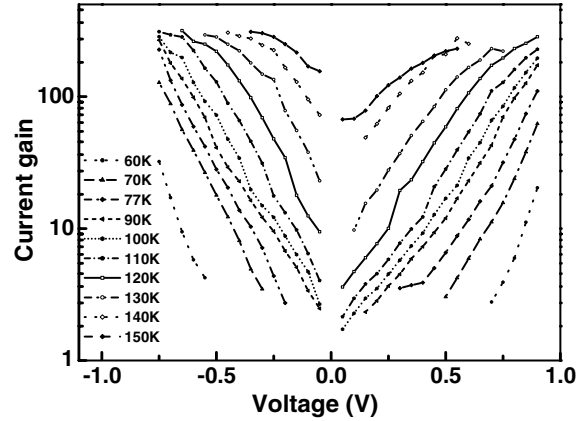


Fig. 5. The current gain of the sample at different voltages and temperatures.

ically within the temperature range. One major difference is that the gain increases without saturation even at 150 K. This shows the change of responsivity is dominated by the current gain thus the capture probability. The capture process is influenced by the repulsive coulomb potential of the extra carriers inside the QDs. Unlike in the QWs, where carriers flow freely in the x – y direction, the isolated charge in the quantum dot could generate potential barrier to electrons passing through the QD layers. That is, why such dependence was never observed in typical QWIPs. In principle, the repulsive potential is related to the capacitor of the QD and the charge number inside the QD. The capture probability P_c of the carriers passing through the QDs could be approximated with the following equation [12]:

$$P_c = P_0 \frac{N_{\text{QD}} - \langle N \rangle}{N_{\text{QD}}} \exp\left(-\frac{e^2 \langle N \rangle}{Ck_B T}\right) \quad \text{with} \quad (2)$$

$$C = 2\epsilon * a_{\text{QD}} / \pi\sqrt{\pi}$$

where P_0 is the capture probability under neutral condition, N_{QD} is the maximum electron number that a QD can accommodate, $\langle N \rangle$ is the average extra carrier number in the QDs. C is the capacitor of the QD and a_{QD} is area of the QD. The number of electrons inside the QDs is determined by the balance of the trapped current into the QDs with the emitted current from the QDs. When the current increases with temperature and voltage, the carrier number inside the QD increases. As a result, the capture probability decreases and the current gain shows a dramatic increase with temperature and bias. To further verify the idea, two QDIPs with identical device structure but different QD doping density was compared. Fig. 6 shows the dark current and the current gain of the two samples at 77 K. The low doping sample showed a much lower dark current as expected. Also, the current gain of the low doping sample is much lower than that of the high doping sample. This phenomenon cannot be explained without the carrier filling process since the identical device structure

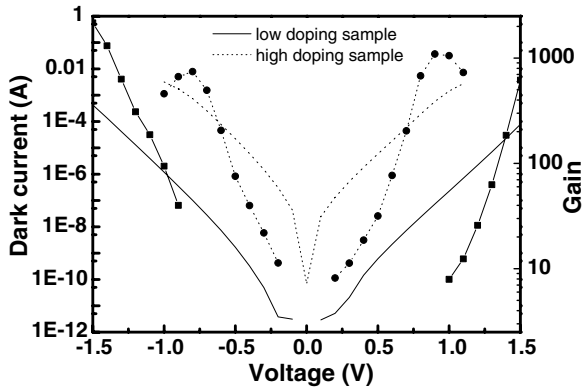


Fig. 6. The dark current and current gain curve for the two samples with different doping concentration at 77 K. The dark current curves were shown by the lines and the measured gain points were shown with the symbols.

should give similar transport property and the current gain value should be similar for the two samples.

With such a concept, the average excess carrier number can be estimated with the measured capture probability and the device parameters. Due to the large size of our QDs, N_{QD} is much larger than $\langle N \rangle$ and $N_{\text{QD}} - \langle N \rangle / N_{\text{QD}}$ is approximated to 1. The neutral capture probability P_0 is equal to the ratio of transit time τ_t and the capture time of the QD τ_c . The transit time can be calculated with the drift velocity

$$\tau_t = \frac{h}{v_d} = \frac{h}{\mu F / [1 + (\mu F / v_{\text{sat}})^2]^{0.5}} \quad (3)$$

where μ is the carrier mobility, v_{sat} is the saturation velocity and h is the height of the QDs. In our calculation, the mobility value of $2000 \text{ cm}^2/\text{V/s}$ and the saturation velocity of $1 \times 10^6 \text{ cm/s}$ were used. The capture time has been reported to be in the order of ps by different experiments [13,14]. Here 5 ps is used in our calculation. Fig. 7 shows the estimated average extra carrier number. When the temperature and bias is low, almost no extra carriers exist in-

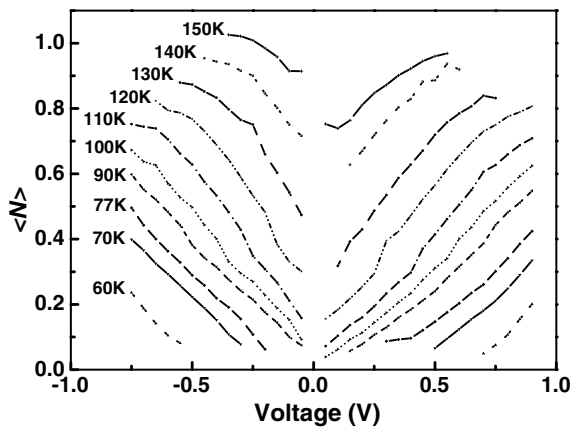


Fig. 7. The calculated average extra carrier number in one QD $\langle N \rangle$ at different temperature and voltages.

side the QDs. When the device current increases with either temperature or voltage, $\langle N \rangle$ could be more than $1e^-$ at 150 K. Due to the higher dark current at negative biases, the extra carrier number is higher under negative biases. Although the dark current increases exponentially with temperature, the average charge in one QD increases only linearly with temperature and voltage. According to the theoretical calculation for the lens shape quantum dot, the energy difference between the ground state and the first excited state energy is around 50 meV for our InAs QDs [15]. Considering the size distribution of the QDs, the density of states of the ground state and the first excited state of the QD layer could overlap and form a band. When the average carrier number increases linearly, the Fermi level of the QD layer also increases in a linear way. The emitted current is thus increases exponentially to balance the captured carriers.

In order to check the reality of the calculated $\langle N \rangle$, we tried to compare the result with the device quantum efficiency. It is well understood that the carrier number inside the QD is essential to the quantum efficiency and the performance of QDIPs. The optimized condition occurs when the ground states are fully occupied and the excited states are all empty, i.e., 2 electrons per QD. Using the measured current gain, the quantum efficiency is calculated with the responsivity and shown in Fig. 8. Due to the increase of the escape probability of the B–B type transition, the quantum efficiency increases exponentially at low bias region in all temperature. However, the peak quantum efficiency decreases by a factor of 10 with the increase of temperature from 70 K to 130 K. Such difference cannot be attributed to the thermal distribution of the carriers inside the QDs which could only change for 10% in our temperature range [3]. Since the doping density of our sample is less than $2e^-/\text{QD}$, as the extra carrier number increases, the quantum efficiency increases and then start to drop slowly. As the temperature goes higher, $\langle N \rangle$ increases and the maximum of the quantum efficiency occurs at lower voltage. If we compare $\langle N \rangle$ with the quantum efficiency carefully as shown in Fig. 9, the peak quantum efficiency happened

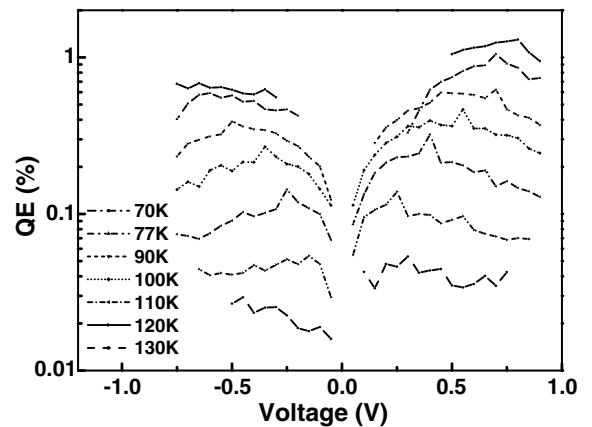


Fig. 8. The quantum efficiency of the sample at different voltages and temperatures.

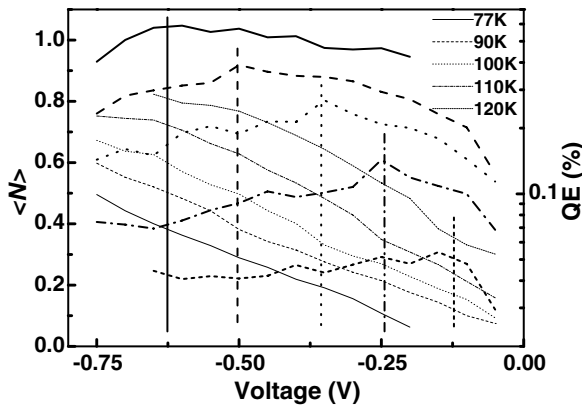


Fig. 9. The quantum efficiency (thick lines) and $\langle N \rangle$ (thin lines) at different temperatures and negative voltages. The vertical lines are used to indicate the voltage of quantum efficiency peaks. The peak quantum efficiency occurs around $\langle N \rangle = 0.4$.

when the excess carrier number is around 0.4 Independent of the temperature. This implied the doping concentration is about $1.6 e^-/\text{QD}$. The number is close to the original doping level and indicating the correctness of the calculated excess carrier number. Since the optimized electron number occurs at lower bias at higher temperature, the escape probability is relatively lower and thus the peak quantum efficiency is lower. Of course, other factors such as the excited carrier life time might also induce the lower quantum efficiency at high temperature.

From the discussion above, we know the change of carrier number inside the QDs plays an important role on the temperature dependence of the responsivity in QDIPs. The higher the dark current is, the more the charge inside the QDs will be. This feature enhances the responsivity and the performance of the QDIPs at higher temperature. The photocurrent can be kept at a higher level with elevated temperature though the quantum efficiency decreases.

Taking the extra charge into account, it is beneficial to use smaller QDs to have a more stable responsivity. The small QDs associated with smaller capacitor could generate higher potential barrier to suppress the carrier injection into the QDs. Moreover, the higher QD density in most of the small size QDs layer provides higher number of state for the captured electrons. The average extra carrier number per QD is less in smaller QDs under the same captured current level. QDIPs with smaller QDs could provide higher current gain and stable quantum efficiency.

4. Summary

The temperature dependence of responsivity of InAs/GaAs QDIPs has been investigated. From the measurement, we found the dramatic change of the current gain with temperature dominates the behavior of the responsivity. The increasing dark current with the temperature injects more carriers inside the QDs. The repulsive potential of the extra carriers suppress the capture process and enhance the current gain. The average extra carrier number calculated from the capture probability qualitatively explained the behavior of the quantum efficiency. From this concept, QDIPs with smaller QD and higher density is predicted to have better temperature stability and also pertain a higher current gain.

Acknowledgement

The work was supported by the National Science Council under contract number NSC94-2112-M-001-042.

References

- [1] D. Pan, E. Towe, S. Kennerly, *Appl. Phys. Lett.* 75 (1999) 2719–2721.
- [2] J. Phillips, P. Bhattacharya, S.W. Kennerly, D.W. Beekman, M. Dutta, *IEEE J. Quantum Electron.* 35 (1999) 936–943.
- [3] H. Lim, W. Zhang, S. Tsao, T. Sills, J. Szafraniec, K. Mi, B. Movaghar, M. Razeghi, *Phys. Rev. B* 72 (2005) 0855332.
- [4] V. Ryzhii, *Semicond. Sci. Technol.* 11 (1996) 759–765.
- [5] S.Y. Wang, S.D. Lin, H.W. Wu, C.P. Lee, *Appl. Phys. Lett.* 78 (2001) 1023–1025.
- [6] Z. Chen, O. Baklenov, E.T. Kim, I. Mukhametzhanov, J. Tie, A. Madhukar, Z. Ye, C. Campbell, *J. Appl. Phys.* 89 (2001) 4558–4563.
- [7] A.D. Stiff, S. Krishna, P. Bhattacharya, S.W. Kennerly, *IEEE J. Quantum Electron.* 37 (2001) 1272–1278.
- [8] S. Chakrabarti, A.D. Stiff-Roberts, P. Bhattacharya, S. Gunapala, S. Bandara, S.B. Rafol, S.W. Kennerly, *IEEE Photonic. Technol. Lett.* 16 (2004) 1361–1363.
- [9] P. Bhattacharya, X.H. Su, S. Chakrabarti, G. Ariyawansa, A.G.U. Perera, *Appl. Phys. Lett.* 86 (2005) 191106.
- [10] Z. Ye, J.C. Campbell, Z. Chen, E. Kim, A. Madhukar, *Appl. Phys. Lett.* 83 (2003) 1234–1236.
- [11] J.Y. Duboz, H.C. Liu, Z.R. Wasilewski, M. Byloss, R. Dudek, *J. Appl. Phys.* 93 (2003) 1320–1322.
- [12] V. Ryzhii, I. Khmyrova, M. Ryzhii, V. Mitin, *Semicond. Sci. Technol.* 19 (2004) 8–16.
- [13] K.W. Sun, A. Kechiantz, B.C. Lee, C.P. Lee, *Appl. Phys. Lett.* 88 (2006) 163117.
- [14] J. Urayama, T.B. Norris, J. Singh, P. Battacharya, *Phys. Rev. Lett.* 86 (2001) 4930–4933.
- [15] O. Stier, M. Grundmann, D. Bimberg, *Phys. Rev. B* 59 (1999) 5688–5701.